LETTER

doi:10.1038/nature10485

Peripheral SMN restoration is essential for long-term rescue of a severe spinal muscular atrophy mouse model

Yimin Hua[1], Kentaro Sahashi[1], Frank Rigo[2], Gene Hung[2], Guy Horev[1], C. Frank Bennett[2] & Adrian R. Krainer[1]

Spinal muscular atrophy (SMA) is a motor neuron disease and the leading genetic cause of infant mortality; it results from loss-of-function mutations in the survival motor neuron 1 (*SMN1*) gene[1]. Humans have a paralogue, *SMN2*, whose exon 7 is predominantly skipped[2], but the limited amount of functional, full-length SMN protein expressed from *SMN2* cannot fully compensate for a lack of *SMN1*. SMN is important for the biogenesis of spliceosomal small nuclear ribonucleoprotein particles[3], but downstream splicing targets involved in pathogenesis remain elusive. There is no effective SMA treatment, but SMN restoration in spinal cord motor neurons is thought to be necessary and sufficient[4]. Non-central nervous system (CNS) pathologies, including cardiovascular defects, were recently reported in severe SMA mouse models and patients[5–8], reflecting autonomic dysfunction or direct effects in cardiac tissues. Here we compared systemic versus CNS restoration of SMN in a severe mouse model[9,10]. We used an antisense oligonucleotide (ASO), ASO-10-27, that effectively corrects *SMN2* splicing and restores SMN expression in motor neurons after intracerebroventricular injection[11,12]. Systemic administration of ASO-10-27 to neonates robustly rescued severe SMA mice, much more effectively than intracerebroventricular administration; subcutaneous injections extended the median lifespan by 25 fold. Furthermore, neonatal SMA mice had decreased hepatic *Igfals* expression, leading to a pronounced reduction in circulating insulin-like growth factor 1 (IGF1), and ASO-10-27 treatment restored IGF1 to normal levels. These results suggest that the liver is important in SMA pathogenesis, underscoring the importance of SMN in peripheral tissues, and demonstrate the efficacy of a promising drug candidate.

To compare the effectiveness of ASO-10-27 delivered centrally versus systemically, we administered an intracerebroventricular (ICV) injection of 20 μg ASO-10-27 on postnatal day 1 (P1) to increase SMN expression in CNS tissues, or we administered a subcutaneous (SC) injection of the ASO on two separate days at 50 μg per g of body weight (μg g^{-1}), between P0 and P3 (two doses). These doses were based on our previous studies with this ASO[11,13]. We also evaluated combined ICV and SC injections, as well as repeated SC injections (Supplementary Table 1). Control heterozygous mice (*Smn*$^{+/-}$ *SMN2*$^{+/0}$) that received ICV and/or SC ASO-10-27 injections had normal survival and behaviour. Severe SMA mice (*Smn*$^{-/-}$ *SMN2*$^{+/0}$) that received ICV and/or SC saline injections survived for 1–2 weeks, with a median survival time of ~10 days, similar to untreated mice (Fig. 1a, Supplementary Figs 1a and 2a, and Supplementary Movie 1). Delivery of the ASO only into the CNS efficiently corrected *SMN2* exon 7 splicing in the spinal cord and led to a striking increase in SMN protein levels, but modestly extended the median survival to 16 days, with a single pup surviving for 1 month (Fig. 1a–c and Supplementary Fig. 2b–d). In marked contrast, systemic treatment with two SC injections resulted in a median survival of 108 days (Fig. 1d). Combining ICV and SC injections of the ASO further increased the median survival to 173 days, and two additional SC injections on P5 and P7, after the initial SC injections at P0–P3, extended the median survival to 137 days (Fig. 1d).

Treated SMA mice varied in size from runts to comparable to their heterozygous littermates; their average weight was low, and their tails were much shorter than normal (Supplementary Figs 3 and 4). The surviving runts slowly gained weight, reaching ~18 g at ~3 months.

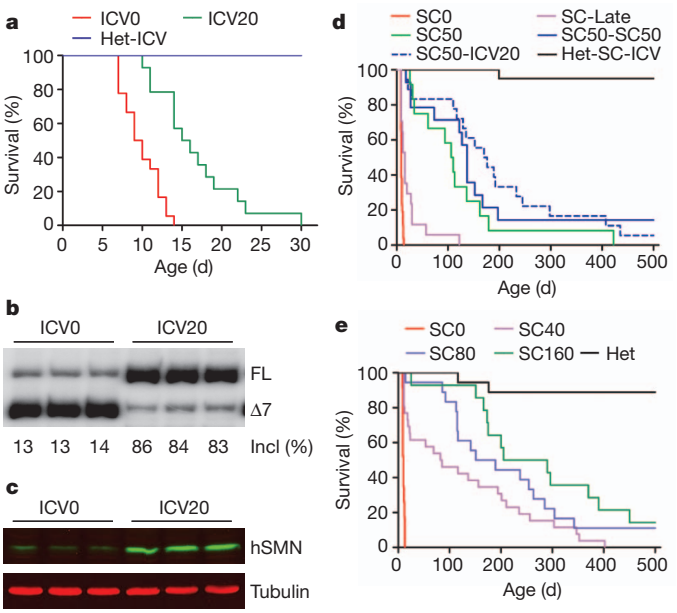

Figure 1 | Systemic versus ICV ASO-10-27 injections in SMA mice. **a**, Survival curves for mice after ICV administration of ASO-10-27 on P1. Administration of 20 μg ASO-10-27 (ICV20, $n = 14$) or saline (ICV0, $n = 18$) resulted in mean survival times of 17 and 10 days (d), respectively ($P < 0.001$). ASO-10-27-treated heterozygotes (Het-ICV, $n = 15$) served as controls. **b**, **c**, Spinal cord RNA and protein samples ($n = 3$) were analysed on P7 by using radioactive RT–PCR (**b**) or immunoblotting with a monoclonal antibody specific for human SMN (hSMN) (**c**). Δ7, exon-7-skipped mRNA; FL, full-length mRNA; incl, exon 7 inclusion; % incl = 100 × Δ7/(FL + Δ7). **d**, Survival curves after SC administration of saline (SC0, $n = 26$) or ASO-10-27 (SC50, $n = 12$) twice between P0 and P3. SC50-SC50 ($n = 14$) mice received two additional SC injections on P5 and P7. Het-SC-ICV ($n = 13$) and SC50-ICV20 ($n = 18$) were heterozygous and SMA mice, respectively, that received combined P1 ICV and P0–P3 SC injections. SC-Late ($n = 17$) were SMA mice that received only two SC injections, on P5 and P7. Each SC injection dose was 50 μg g^{-1} body weight. $P < 0.0001$ for all groups versus SC0 except for SC-Late, $P < 0.05$. **e**, Dose-dependent survival after two SC injections at P0–P3 with 40 (SC40, $n = 26$), 80 (SC80, $n = 18$) or 160 (SC160, $n = 14$) μg g^{-1} of ASO-10-27. Saline-treated SMA (SC0, $n = 23$) or heterozygous mice (Het, $n = 18$) served as controls. $P < 0.0001$ for all groups versus SC0.

[1]Cold Spring Harbor Laboratory, PO Box 100, Cold Spring Harbor, New York 11724, USA. [2]Isis Pharmaceuticals, 2855 Gazelle Court, Carlsbad, California 92010, USA.

Most rescued SMA mice could run and climb normally; however, their tails and ears developed necrosis and were gradually lost, resembling the phenotype of type III SMA mice (Supplementary Fig. 3e, f). Additional delivery of the ASO either by ICV injection on P1 or repeat SC injections on P5 and P7 delayed necrosis (Supplementary Fig. 3g).

To further characterize the effects of the ASO administered systemically, we carried out a dose–response study with 0 (SC0), 40 (SC40), 80 (SC80) and 160 (SC160) $\mu g\,g^{-1}$ ASO-10-27 as an SC injection, given twice between P0 and P3. Systemic treatment with the ASO resulted in a dose-dependent increase in survival (Fig. 1e), with the median survival increasing from 10 days to 84, 170 and 248 days, respectively. At the highest dose tested, the ASO given systemically resulted in long-term survival comparable to the best results achieved by adeno-associated virus expression of the SMN protein in a slightly less severe mouse model[14–16]. Remarkably, 2 of 14 mice in the SC160 group and 2 of 18 in the SC80 group are still alive and active after >500 days. A similar survival benefit was achieved by intraperitoneal administration (Supplementary Fig. 5). There was no significant difference in weight gain among the three SC-dosing groups; however, mice in the SC160 group had significantly longer tails (Supplementary Fig. 6a–e). We also observed dose-dependent rescue of ear and tail necrosis and dose-dependent delays in the development of cataracts and rectal prolapse (Supplementary Fig. 6f–h). Administration of the ASO in two doses on P5 and P7 resulted in a modest increase in survival, compared with earlier treatment (between P0 and P3), emphasizing the importance of early postnatal therapeutic intervention (Fig. 1d).

To examine *SMN2* splicing changes in various tissues after SC injection of the ASO, we performed reverse transcription followed by PCR (RT–PCR) on RNA samples from P7 mice. We detected a dose-dependent increase in exon 7 inclusion in the spinal cord, brain, liver, heart, kidneys and skeletal muscle, with the strongest effect occurring in the liver and the weakest in the kidneys (Fig. 2a, b and Supplementary Fig. 7a, b). By contrast, ICV administration of the ASO resulted in a much more robust change in exon 7 inclusion in the brain and spinal cord tissues but had very limited effects in peripheral tissues (Supplementary Fig. 8a). Immunoblotting of spinal cord, liver and heart tissue samples from mice treated by SC administration showed a corresponding increase in full-length SMN protein (Fig. 2c and Supplementary Figs 7c and 8b). Exon 7 inclusion in the liver significantly decreased after P30 (Fig. 2d, e and Supplementary Fig. 9), consistent with the measured half-life of the ASO being 22 days in the liver (data not shown). These data suggest that transiently increasing SMN expression in peripheral tissues during the first few weeks of life has a profound effect on long-term survival of severe SMA mice.

The *SMN2*-splicing changes were consistent with the ASO distribution, as assayed by immunohistochemistry, with the apparent exception of the kidneys; however, in the kidneys, most of the ASO had not been internalized by the cells (Supplementary Figs 10 and 11). We also observed some of the ASO accumulating in spinal cord motor neurons (Supplementary Figs 10 and 11). The limited distribution of the ASO and the moderate *SMN2*-splicing changes in the CNS after systemic administration probably reflect incomplete closure of the blood–brain barrier in neonates[17] and/or retrograde transport of the ASO. However, we detected strong cytoplasmic SMN staining and/or a pronounced increase in gem number in spinal cord motor neurons after ICV injection of 20 μg ASO-10-27 but not after two SC injections of ASO-10-27 at 80 $\mu g\,g^{-1}$ between P0 and P3, a dosage that substantially rescued the severe SMA mice (Supplementary Figs 12 and 13). Therefore, the effect on splicing in the CNS after systemic administration probably contributes to the extended survival, which is consistent with the combined ICV and SC treatment resulting in even better survival than SC administration alone (Fig. 1d). However, the striking effects of systemic administration on survival in this severe mouse model cannot be explained solely by a direct effect on *SMN2* splicing in the CNS.

The rescue of severe SMA mice by systemic administration of, for example, histone deacetylase inhibitors or adeno-associated virus

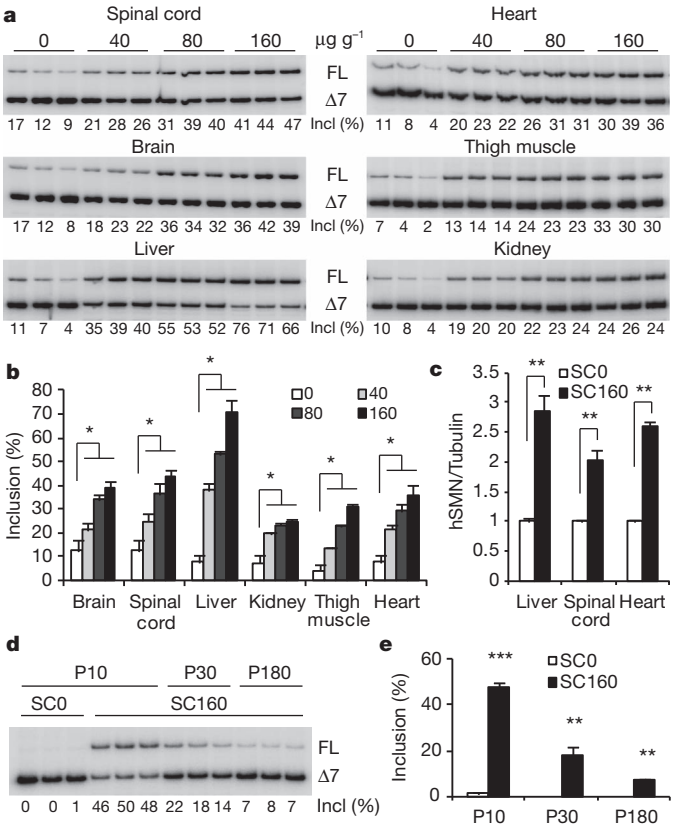

Figure 2 | *SMN2* splicing and protein expression in mouse tissues after SC injection of ASO-10-27. **a**, Tissue RNA samples from SMA mice were analysed by radioactive RT–PCR at P7 after two SC injections between P0 and P3 with 0, 40, 80 or 160 $\mu g\,g^{-1}$ body weight ASO-10-27. **b**, Histogram of exon 7 inclusion data from panel **a** ($n = 3$). **c**, Protein samples from P7 SMA mice ($n = 3$) that had been treated with 160 $\mu g\,g^{-1}$ body weight ASO-10-27 were analysed by immunoblotting with a monoclonal antibody specific for human SMN (see also Supplementary Fig. 8b). **d**, RT–PCR of liver RNA from P10, P30 and P180 SMA mice, showing the decreasing effect of ASO-10-27 over time. **e**, Histogram of data from panel **d**. **b**, **c**, **e**, Data are presented as mean + s.d. *, $P < 0.05$; **, $P < 0.01$; ***, $P < 0.0001$; all compared with saline controls.

vectors, has been attributed to the ability of these agents to cross the blood–brain barrier[10,15]. However, our data indicate that SMN restoration in peripheral tissues, in combination with partial restoration in the CNS, can achieve efficient rescue of severe SMA mice.

In mice that had been treated systemically with 160 $\mu g\,g^{-1}$ ASO-10-27 and sacrificed on P9, histological examination of tissues or organs associated with SMA revealed striking improvements, consistent with the markedly increased survival of mice in the SC160 group. The α-motor neuron counts in the spinal cords of these mice were comparable to those of the control heterozygous littermates, and the mean area of muscle fibre cross-sections was >80% of that of heterozygotes (Fig. 3a, b and Supplementary Fig. 14a). Likewise, the heart weight and the thickness of the interventricular septum and the left ventricular wall were similar in mice in the SC160 group and their heterozygous littermates (Fig. 3c, d and Supplementary Fig. 14b). Finally, staining of the neuromuscular junctions (NMJs) showed that NMJ integrity was similar in mice in the SC160 group and their heterozygous littermates (Fig. 3e).

Most of the mice that were treated systematically with the ASO showed no overt signs of motor dysfunction (Supplementary Movie 2 and Supplementary Table 2). We used three tests to evaluate behaviour and motor function. The first was a rotarod test, which requires limb muscle strength, as well as balance and coordination. Three-month-old mice in the SC80 and SC160 groups could stay on the rotating rod for ~12 s: that is, for less time than the control heterozygotes but for longer

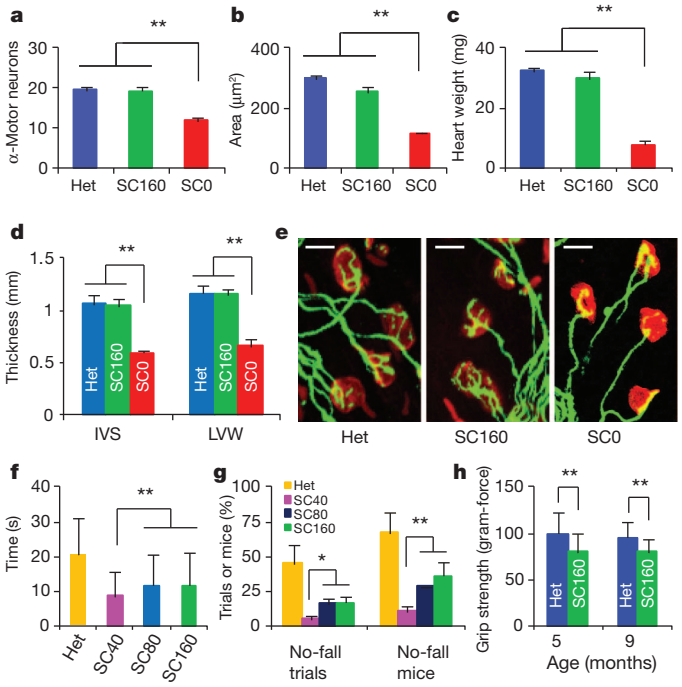

Figure 3 | Evaluation of affected tissues and motor function. Tissues from three groups of P9 mice were stained with haematoxylin and eosin: SMA mice that had been treated with ASO-10-27 (SC160, two SC injections at 160 μg g^{-1} body weight at P0–P3, $n = 6$), saline controls (SC0, $n = 6$) and untreated heterozygotes (Het, $n = 6$) (see also Supplementary Fig. 14). Saline-treated mice were ambulant at P9 and were expected to live for another 3–5 days. α-Motor neuron counts in each cross-section of the L1–L2 spinal cord (**a**), mean fibre cross-sectional area (for a total of 200 fibres) of the rectus femoris muscle (**b**), heart weight (**c**) and thickness of the heart interventricular septum (IVS) and left ventricular wall (LVW) (**d**) significantly improved in ASO-10-27-treated mice. **e**, The arborization complexity of NMJs was restored in ASO-10-27-treated mice (red, endplates; green, neurofilament medium). Scale bar, 10 μm. **f**, **g**, P90 SC40 ($n = 12$, 124 trials), SC80 ($n = 13$, 137 trials), SC160 ($n = 11$, 117 trials) and untreated heterozygous (Het, $n = 12$, 135 trials) mice were tested three to five times per day for 3 days on a rotarod, using an acceleration profile. The mean times for staying on the spinning rod (**f**) and the percentage of no-fall trials and of mice with ≥1 no-fall trial (**g**) are shown. **h**, The grip strength (gram-force) of SC160 mice ($n = 6$) evaluated at 5 and 9 months reached ~80% of that of heterozygous mice ($n = 6$). **a**–**d**, **f**–**h**, Data are presented as mean + s.d. *, $P < 0.05$; **, $P < 0.01$.

than mice in the SC40 group. Some ASO-10-27-treated mice passed a 30 s acceleration-profile test that many of the heterozygotes failed (Fig. 3f, g and Supplementary Movie 3). Considering that SMA is a neuromuscular disease, this performance represents a remarkable phenotypic improvement. The second test evaluated muscle strength in mice from the SC160 group at 5 and 9 months. At both ages, the forelimb grip strength of treated SMA mice was ~80% that of the control heterozygous mice (Fig. 3h). The final test used HomeCageScan, a video-based platform for automated high-resolution behaviour analysis[18]. ASO-10-27-treated SMA mice performed various behaviours similarly to control heterozygous mice, except for rearing, suggesting some hindlimb weakness (Supplementary Fig. 15).

Two observations prompted us to examine the growth hormone (GH)–IGF1 axis. First, all severe SMA mice are small[9,10,19], reflecting growth retardation (Supplementary Figs 2a and 3c). Second, the major effect of SC injection of the ASO on *SMN2* splicing is in the liver, which contributes ~75% of the circulating IGF1 (ref. 20). Moreover, restoring IGF1 expression in the liver is sufficient to support normal postnatal growth of *Igf1*-null mice[20]. IGF1 is a potent neurotrophic factor[21] and is also involved in cardiac development and function[22]. An enzyme-linked immunosorbent assay (ELISA) of serum samples from SMA mice at P6–P9 showed that IGF1 was undetectable or present at greatly reduced levels compared with the heterozygous controls; SC administration of the ASO restored IGF1 to normal levels in SMA mice (Fig. 4a).

RT–PCR showed that the level of hepatic *Igf1* messenger RNA was not reduced in SMA mice compared with the heterozygous controls and that it increased from P1 to P5 in both SMA and control mice (Fig. 4b). IGF-binding protein, acid labile subunit (IGFALS), which is postnatally stimulated by GH, binds to IGF1 and IGF-binding protein 3 (IGFBP3) to form a stable ternary complex, extending the half-life of IGF1 from 10 min to >12 h[23]. The inactivation of *Igfals* results in low levels of circulating IGF1 and IGFBP3, as well as impaired postnatal growth[23]. RT–PCR revealed a marked reduction in the amount of *Igfals* mRNA in the liver of both P1 and P5 SMA mice compared with the heterozygous controls; moreover, administration of the ASO rescued *Igfals* expression (Fig. 4c, d). We conclude that the striking reduction in serum IGF1 levels in SMA mice is likely to be caused by decreased *Igfals* expression, which correlates with SMN deficiency and SMA progression.

Because *Igfals* expression is decreased on P1, when the pups are still healthy, we propose that the early deficiency in circulating IGF1 may be one of the factors that contribute to the pathogenesis of severe SMA mice (Supplementary Fig. 1b). Although in several mouse mutants, an impaired GH–IGF1 axis results in an increased lifespan[24], a severe lack of IGF1 may contribute to SMA progression, together with other defective factors. Consistent with our hypothesis, two recent studies have shown that a local increase in IGF1 in either the spinal cord or muscle increases the survival of severe SMA mice[25,26]. Indeed, disruption of the IGF1 system is a common feature of neurodegenerative diseases, including Alzheimer's disease and amyotrophic lateral sclerosis (ALS)[27]. *Igf1*-null mice also show some phenotypic similarity to SMA mice, such as small size and severe and generalized muscle dystrophy (including of the diaphragm and heart), with most of them dying at birth[28]. Moreover, dysregulation of the IGF1 receptor and its downstream signalling pathway has been observed in patients with type I SMA[29]. However, the results of IGF1 therapy for ALS are not consistent between mice and humans[21,30]. In light of this inconsistency,

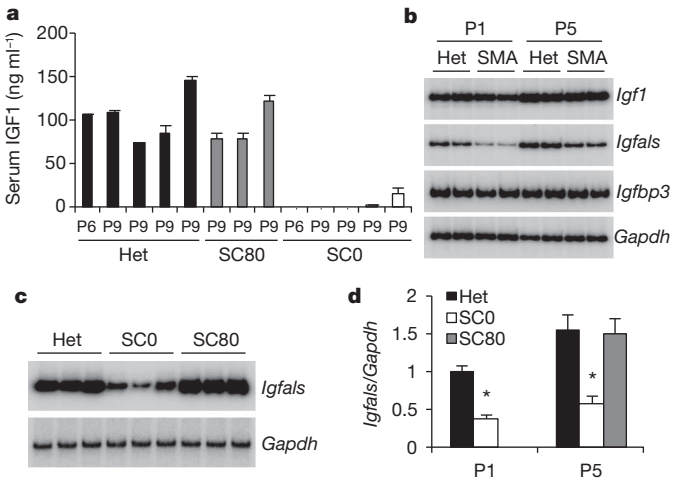

Figure 4 | The IGF1 system is disrupted in SMA mice. Treated SMA mice (SC80) received two SC injections of ASO-10-27 at 80 μg g^{-1} body weight between P0 and P3. **a**, IGF1 serum levels in P6 and P9 SMA mice (SC0), as measured by ELISA (mean of three measurements per sample), were strikingly lower than for their heterozygous littermates (Het) or treated SMA mice ($P < 0.001$ for all samples). **b**, Total liver RNA from P1 and P5 SMA mice and their heterozygous littermates was analysed by radioactive RT–PCR to measure *Igf1*, *Igfals* and *Igfbp3* expression, with *Gapdh* as a control. **c**, ASO-10-27 treatment restored hepatic *Igfals* expression at P5, as shown by radioactive RT–PCR. **d**, Quantification of hepatic *Igfals* expression ($n = 5$). *, $P < 0.01$ versus samples from heterozygous littermates or ASO-10-27-treated SMA mice. **a**, **d**, Data are presented as mean + s.d.

it will be crucial to determine the extent to which SMA mouse models accurately mimic human SMA. This will further refine our understanding of the mouse models and influence the development of therapeutics and clinical treatments for SMA.

METHODS SUMMARY

ASO-10-27 was synthesized as described previously[11] and dissolved in 0.9% saline. The severe SMA mouse model was generated from a type III SMA mouse model, as described previously[9,10]. All mouse protocols were in accordance with the Cold Spring Harbor Laboratory's Institutional Animal Care and Use Committee guidelines. Treated mice (control and ASO-10-27) were provided with additional gel food. The procedures for neonatal ICV injection, tissue sample collection, RT–PCR, western blotting and the human-specific anti-SMN antibody (SMN-KH) were as described previously[11]. The primers for the gene expression analysis are shown in Supplementary Table 3. Serum IGF1 levels were analysed with a Mouse/Rat IGF-I Quantikine ELISA kit (R&D Systems).

Mouse spinal cords, quadriceps and hearts were fixed and stained with haematoxylin and eosin as described previously[12]. α-Motor neurons were counted in serial 10–20-μm cross-sections of the lumbar (L1–L2) spinal cord. The muscle fibre cross-sectional area was calculated by using AxioVision LE velocity software. NMJ staining *in toto* was performed as described previously[12].

For the rotarod (AccuScan Instruments) test, a four-phase profile was used: phase 1, from 1 to 10 r.p.m. in 7.5 s; phase 2, from 10 to 0 r.p.m. in 7.5 s; phase 3, from 0 to 10 r.p.m. in 7.5 s in the opposite direction; and phase 4, from 10 to 0 r.p.m. in 7.5 s. A grip-strength meter (Columbus Instruments) was used for the gripping test. Mice were allowed to grasp a triangular bar with their forelimbs and were pulled back horizontally. The test was repeated five times for each mouse, and the highest value was recorded as the grip force for that animal.

Statistical significance was analysed by two-tailed Student's *t*-tests. Kaplan–Meier survival data were analysed with Mantel–Cox tests using the program GraphPad Prism.

Received 15 April; accepted 18 August 2011.

1. Lefebvre, S. *et al.* Identification and characterization of a spinal muscular atrophy-determining gene. *Cell* **80,** 155–165 (1995).
2. Lorson, C. L., Rindt, H. & Shababi, M. Spinal muscular atrophy: mechanisms and therapeutic strategies. *Hum. Mol. Genet.* **19,** R111–R118 (2010).
3. Burghes, A. H. & Beattie, C. E. Spinal muscular atrophy: why do low levels of survival motor neuron protein make motor neurons sick? *Nature Rev. Neurosci.* **10,** 597–609 (2009).
4. Gavrilina, T. O. *et al.* Neuronal SMN expression corrects spinal muscular atrophy in severe SMA mice while muscle-specific SMN expression has no phenotypic effect. *Hum. Mol. Genet.* **17,** 1063–1075 (2008).
5. Rudnik-Schoneborn, S. *et al.* Congenital heart disease is a feature of severe infantile spinal muscular atrophy. *J. Med. Genet.* **45,** 635–638 (2008).
6. Bevan, A. K. *et al.* Early heart failure in the SMNΔ7 model of spinal muscular atrophy and correction by postnatal scAAV9-SMN delivery. *Hum. Mol. Genet.* **19,** 3895–3905 (2010).
7. Heier, C. R., Satta, R., Lutz, C. & DiDonato, C. J. Arrhythmia and cardiac defects are a feature of spinal muscular atrophy model mice. *Hum. Mol. Genet.* **19,** 3906–3918 (2010).
8. Shababi, M. *et al.* Cardiac defects contribute to the pathology of spinal muscular atrophy models. *Hum. Mol. Genet.* **19,** 4059–4071 (2010).
9. Gogliotti, R. G., Hammond, S. M., Lutz, C. & Didonato, C. J. Molecular and phenotypic reassessment of an infrequently used mouse model for spinal muscular atrophy. *Biochem. Biophys. Res. Commun.* **391,** 517–522 (2010).
10. Riessland, M. *et al.* SAHA ameliorates the SMA phenotype in two mouse models for spinal muscular atrophy. *Hum. Mol. Genet.* **19,** 1492–1506 (2010).
11. Hua, Y. *et al.* Antisense correction of *SMN2* splicing in the CNS rescues necrosis in a type III SMA mouse model. *Genes Dev.* **24,** 1634–1644 (2010).
12. Passini, M. A. *et al.* Antisense oligonucleotides delivered to the mouse CNS ameliorate symptoms of severe spinal muscular atrophy. *Sci. Transl. Med.* **3,** 72ra18 (2011).
13. Hua, Y., Vickers, T. A., Okunola, H. L., Bennett, C. F. & Krainer, A. R. Antisense masking of an hnRNP A1/A2 intronic splicing silencer corrects *SMN2* splicing in transgenic mice. *Am. J. Hum. Genet.* **82,** 834–848 (2008).
14. Passini, M. A. *et al.* CNS-targeted gene therapy improves survival and motor function in a mouse model of spinal muscular atrophy. *J. Clin. Invest.* **120,** 1253–1264 (2010).
15. Foust, K. D. *et al.* Rescue of the spinal muscular atrophy phenotype in a mouse model by early postnatal delivery of SMN. *Nature Biotechnol.* **28,** 271–274 (2010).
16. Dominguez, E. *et al.* Intravenous scAAV9 delivery of a codon-optimized *SMN1* sequence rescues SMA mice. *Hum. Mol. Genet.* **20,** 681–693 (2011).
17. Ek, C. J., Habgood, M. D., Dziegielewska, K. M. & Saunders, N. R. Structural characteristics and barrier properties of the choroid plexuses in developing brain of the opossum (*Monodelphis domestica*). *J. Comp. Neurol.* **460,** 451–464 (2003).
18. Steele, A. D., Jackson, W. S., King, O. D. & Lindquist, S. The power of automated high-resolution behavior analysis revealed by its application to mouse models of Huntington's and prion diseases. *Proc. Natl Acad. Sci. USA* **104,** 1983–1988 (2007).
19. Park, G. H., Kariya, S. & Monani, U. R. Spinal muscular atrophy: new and emerging insights from model mice. *Curr. Neurol. Neurosci. Rep.* **10,** 108–117 (2010).
20. Wu, Y., Sun, H., Yakar, S. & LeRoith, D. Elevated levels of insulin-like growth factor (IGF)-I in serum rescue the severe growth retardation of IGF-I null mice. *Endocrinology* **150,** 4395–4403 (2009).
21. Kaspar, B. K., Llado, J., Sherkat, N., Rothstein, J. D. & Gage, F. H. Retrograde viral delivery of IGF-1 prolongs survival in a mouse ALS model. *Science* **301,** 839–842 (2003).
22. Colao, A. The GH–IGF-I axis and the cardiovascular system: clinical implications. *Clin. Endocrinol.* **69,** 347–358 (2008).
23. Domené, H. M. *et al.* Human acid-labile subunit deficiency: clinical, endocrine and metabolic consequences. *Horm. Res.* **72,** 129–141 (2009).
24. Kenyon, C. The plasticity of aging: insights from long-lived mutants. *Cell* **120,** 449–460 (2005).
25. Shababi, M., Glascock, J. & Lorson, C. L. Combination of *SMN trans*-splicing and a neurotrophic factor increases the life span and body mass in a severe model of spinal muscular atrophy. *Hum. Gene Ther.* **22,** 135–144 (2011).
26. Bosch-Marce, M. *et al.* Increased IGF-1 in muscle modulates the phenotype of severe SMA mice. *Hum. Mol. Genet.* **20,** 1844–1853 (2011).
27. Trejo, J. L., Carro, E., Garcia-Galloway, E. & Torres-Aleman, I. Role of insulin-like growth factor I signaling in neurodegenerative diseases. *J. Mol. Med.* **82,** 156–162 (2004).
28. Powell-Braxton, L. *et al.* IGF-I is required for normal embryonic growth in mice. *Genes Dev.* **7,** 2609–2617 (1993).
29. Millino, C. *et al.* Different atrophy-hypertrophy transcription pathways in muscles affected by severe and mild spinal muscular atrophy. *BMC Med.* **7,** 14 (2009).
30. Sorenson, E. J. *et al.* Subcutaneous IGF-1 is not beneficial in 2-year ALS trial. *Neurology* **71,** 1770–1775 (2008).

Supplementary Information is linked to the online version of the paper at www.nature.com/nature.

Acknowledgements We gratefully acknowledge support from the Muscular Dystrophy Association, the National Institute of General Medical Sciences and St. Giles Foundation. We thank J. Bu and M. Passini for protocols and advice on NMJ staining, and S. Hearn for assistance with microscope imaging.

Author Contributions Y.H., A.R.K. and C.F.B. designed the study and wrote the paper. Y.H., K.S., F.R., G. Hung and G. Horev carried out the experiments and analysed the data. All authors read the manuscript.

Author Information Reprints and permissions information is available at www.nature.com/reprints. The authors declare competing financial interests: details accompany the full-text HTML version of the paper at www.nature.com/nature. Readers are welcome to comment on the online version of this article at www.nature.com/nature. Correspondence and requests for materials should be addressed to A.R.K. (Krainer@cshl.edu).